British Journal of Applied Science & Technology
3(2): 340-349, 2013

SCIENCEDOMAIN *international*
www.sciencedomain.org

Studies on the Optical and Electrical Properties of 4-Methoxybenzoin NLO Single Crystal

Sagadevan Suresh[1*]

[1]*Crystal Growth Centre, Anna University, Chennai-25, India.*

Author's contribution

This work was carried out only by author SS. The author SS read and approved the final manuscript.

Research Article

Received 16th November 2012
Accepted 24th January 2013
Published 3rd March 2013

ABSTRACT

Organic nonlinear optical single crystals of 4-methoxy benzoin were grown by slow evaporation technique. The X-ray diffraction analysis revealed that 4-methoxy benzoin single crystals belong to orthorhombic crystal system with a space group $Pca2_1$.Optical absorption range of the grown crystal was measured by UV-VIS-NIR spectrophotometer. The optical absorbance spectrum of 4-methoxy benzoin crystal has been used to calculate the optical band gap (E_g), absorption coefficient (α), refractive index (n), and the real (ε_r) and imaginary (ε_i) components of the dielectric constant. The DC electrical conductivity measurements were carried out for the crystals using the conventional two – probe technique. The conductivity study indicates that the DC conductivity of the samples increase with the increase in temperature. The activation energies were also calculated from DC conductivity studies. Photoconductivity measurements carried out on the grown crystal reveal the negative photoconducting nature.

Keywords: Solution growth; NLO; Single crystal XRD; UV-VIS-NIR spectra; Refractive index; Reflectance; DC electrical conductivity and Photoconductivity studies.

1. INTRODUCTION

The growth of optical devices, such as photonic integrated circuitry, depends strongly on the design of extremely efficient nonlinear optical (NLO) materials. Among such NLO materials,

**Corresponding author: E-mail: sureshsagadevan@yahoo.co.in;*

organic materials are shown to be superior to their inorganic counterparts in terms of synthesis, crystal fabrication, potential to make large devices and very much faster optical nonlinearities [1,2].Organic derivatives possessing polarizable electrons spread out over a prominent distance with various combinations of terminal electron donor and/or acceptor groups have been the objective of recent research, particularly in view of their large molecular hyperpolarizability and good crystallizability [7-11], which may contribute to a wide range of applications in integrated optics (second harmonic generation (SHG), frequency mixing, electro-optic modulation, parametric effects, etc.) [12,13]. The design and synthesis of organic molecules exhibiting second-order nonlinear optical (NLO) properties has also been prompted by their enormous potential for application in optical communications, optical computing, data storage, dynamic holography, harmonic generators, frequency mixing and optical switching [10,14].The synthesis, structural, vibrational, optical and second harmonic generation (SHG) properties of single crystals of 4-methoxy benzoin have been reported earlier [15]. The present investigation, deals with the growth of 4-methoxy benzoin single crystals by slow evaporation technique. The grown single crystals were subjected to single crystal X-ray diffraction, optical properties, DC electrical conductivity and photoconductivity studies. The results of these investigations are discussed.

2. MATERIAL AND METHOD

Single crystals of 4-methoxy benzoin, an organic nonlinear optical material have been grown by a slow evaporation technique at room temperature. The defect-free, optically clear, and perfectly shaped tiny crystals were chosen as seeds for the growth experiment. From XRD studies, it is confirmed that 4-methoxy benzoin belongs to orthorhombic crystal structure with space group $Pca2_1$. The single crystalline nature is thus confirmed and the space group reveals that the material shows no inversion symmetry (non-centrosymmetric). Optical absorption measurements were made using Perkin Elmer Lamda 35 UV-VIS-NIR spectrophotometer with a resolution of 2 nm in the region from 200 nm to 1000 nm to measure the absorption range of the crystal. The samples (rectangular shaped crystals) were cut parallel to the cleavage plane to the desired thickness of 1-2 mm and polished using silicon carbide paper. They were annealed for two hours at 150ºC to remove moisture content, if present. Opposite faces of the sample crystals were coated with good quality graphite to obtain a good ohmic contact with the electrodes. The samples were again annealed in the holder assembly at 150ºC before making observations. The resistance of the crystal was measured using a megohmmeter. The observations were made while cooling the sample and temperature was controlled to an accuracy of ± 1ºC. The dimensions of the crystal were measured using a travelling microscope. The crystal sample is well-polished and surfaces are cleaned with acetone. This is attached to a microscope slide and two electrodes of thin copper wire (0.14 cm diameter) are fixed onto the specimen at some distance apart using silver paint. After this it is annealed at a temperature of 100ºC to perfect dryness. A D.C. power supply, a Keithley 485 picoammeter and the prepared sample are connected in series. The applied field is increased from 0 to 900 Vcm^{-1}. The sample is covered with a black cloth to avoid exposure to any radiation. The current (dark) is measured. To measure the photoconductivity, light from a 100 W halogen lamp is focused onto the sample. The current is noted for varying applied fields as before.

3. RESULTS AND DISCUSSION

3.1 Single Crystal XRD

The lattice parameters were found to be a=14.45 Á, b=14.08 Á, C=5.85 Á, α = β = γ = 90° with unit cell volume V = 1192.62 $Á^3$. From the data, it is observed that the grown crystal is belongs to orthorhombic system and space group $Pca2_1$. These lattice parameters values are found to be in good agreement with the reported values [15].

3.2 Optical Studies

UV-VIS-NIR absorption spectrophotometer was used to record the absorption spectrum in the range between 200 nm and 1000 nm. From the observed spectrum (Fig. 1), the lower cut-off wavelength is found to be 400 nm. The absence of absorption in the near infrared region provides the access to the laser wavelength of 1064 nm from Nd: YAG source for second harmonic generation. Hence, UV absorption studies reveal that the grown 4-methoxy benzoin crystal is one of the suitable materials for exhibiting second harmonic generation in the entire visible and near infrared region. The measured transmittance (T) was used to calculate the absorption coefficient (α) using the relation,

$$\alpha = \frac{2.3026 \log\left(\frac{1}{T}\right)}{t} \tag{1}$$

where T is the transmittance and t is the thickness of the crystal. Optical band gap (E_g) was evaluated from the absorption spectrum and optical absorption coefficient (α) near the absorption edge is given by,

$$\alpha h\nu = A(h\nu - E_g)^{1/2} \tag{2}$$

where E_g is the optical band gap of the crystal and A is a constant. The Tauc's plot of $(\alpha h\nu)^2$ against the photon energy (hν) at room temperature (Fig. 2) shows a linear behaviour, (α-absorption coefficient and h-Planck's constant) which can be considered as an evidence of the indirect transition. Hence, assuming indirect transition between valence band and conduction band, the bandgap (E_g) is estimated by extrapolation of the linear portion of the curve to the point $(\alpha h\nu)^2 = 0$ [16].Using this method, the band gap of the 4-methoxy benzoin crystal was found to be 3.50 eV. As a consequence of wide band gap, the grown crystal has large transmittance in the visible region [17].

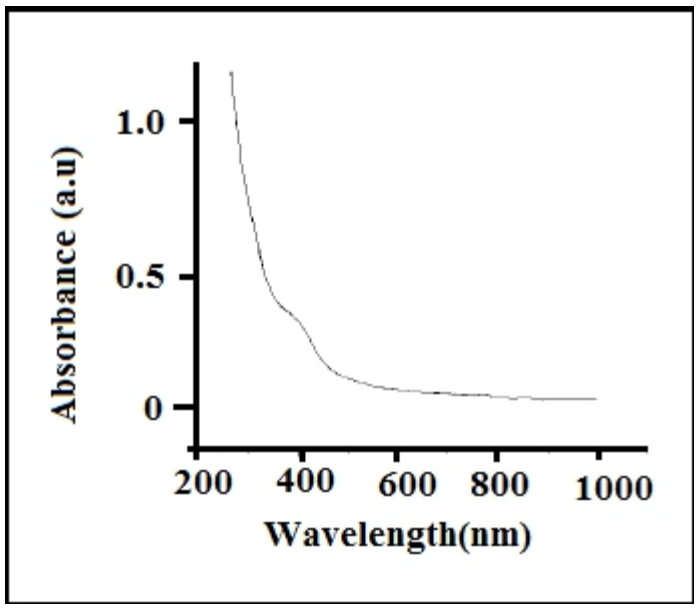

Fig. 1. UV-VIS-NIR absorption spectrum of 4-methoxy benzoin crystal

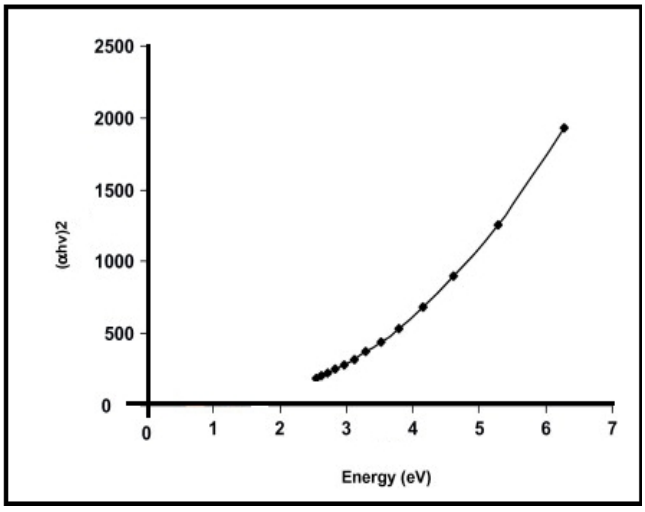

Fig. 2. Band gap of 4-methoxy benzoin crystal

Extinction coefficient (K) can be obtained from the following equation:

$$K = \frac{\lambda \alpha}{4\pi} \tag{3}$$

The transmittance (T) is given by

$$T = \frac{(1-R)^2 \exp(-\alpha t)}{1-R^2 \exp(-2\alpha t)} \tag{4}$$

Reflectance (R) in terms of absorption coefficient can be obtained from the above equation. Hence,

$$R = 1 \pm \frac{\sqrt{1-\exp(-\alpha t)+\exp(\alpha t)}}{1-\exp(-\alpha t)} \tag{5}$$

Refractive index (n) can be determined from reflectance data using the following equation

$$n = -(R+1) \pm 2\frac{\sqrt{R}}{(R-1)} \tag{6}$$

The refractive index (n) is 1.79 at λ =1000 nm. From the optical constants, electric susceptibility (χ_c) can be calculated according to the following relation [18].

$$\varepsilon_r = \varepsilon_0 + 4\pi\chi_C = n^2 - k^2 \tag{7}$$

Hence,

$$\chi_C = \frac{n^2 - k^2 - \varepsilon_0}{4\pi} \tag{8}$$

where ε_0 is the dielectric constant in the absence of any contribution from free carriers. The value of electric susceptibility χ_C is 0.131 at λ =1000 nm. The real part dielectric constant ε_r and imaginary part dielectric constant ε_i can be calculated from the following relations [19].

$$\varepsilon_r = n^2 - k^2 \quad \& \quad \varepsilon_i = 2nk \tag{9}$$

The value of real ε_r and ε_i imaginary dielectric constants at λ =1000 nm are 1.261 and 5.864 x 10^{-5} respectively.

3.3 DC Conductivity Studies

There are three mechanisms of electrical conduction dielectrics (depending on the type of carriers) (a) ionic or electronic conduction (b) mol ionic or electrophoretic conduction and (c) electronic conduction. Dielectrics actually exhibit a combined conduction, especially ionic and electronic conduction. Ionic conductivity studies provide valuable information about the state of point imperfections. At any particular temperature, the Gibb's free energy of a crystal is minimum when a certain fraction of ions occupy the normal lattice. As the temperature rises, more and more defects are produced which, in turn, increases the conductivity. In the high temperature (intrinsic) region, the effect of impurity on electrical conduction will not change appreciably whereas in the low temperature (extrinsic) region the presence of impurity in the crystal increases its conductivity. The electrical conduction in dielectrics is mainly a defect controlled process in the low temperature region. The presence of impurities and vacancies mainly determine this region. The energy needed to form the defect is much

larger than the energy needed for its drift. The conductivity of the crystal in the high temperature region is determined by the intrinsic defects caused by thermal fluctuations in the crystal. Conduction in an ionic crystal is, in general, a defect controlled property. The defect concentration increases exponentially with rise of temperature and the electrical conductivity increases correspondingly. Addition of divalent impurities to the crystal influences the concentration of point defects. Processes like association, aggregation and precipitation which become important at low temperatures and higher impurity levels, in general, reduce the free point defects that are necessary for electrical conduction. Formation, migration and association of point defects are governed by characteristic activation energies. An analytical increase in the concentration of defects both through the law of mass action and charge neutrality criterion. With the usual electric field, the charge transport by electrons in ionic crystals is zero because of a large forbidden gap. Ionic conduction occurs either through the migration of positive and negative ions in an external electric field (the ions originate either in the material in question or in interstitial impurities) or through the motion of ions in vacancies which reflects the migration of vacancies. If the sample is placed in a stationary electric field, the carriers may be considered to be contained in an enclosure bounded by the capacitor plates. As the carriers may not leave the enclosure they accumulate in the regions close to the plates which cause a concentration gradient to be formed and this gradient feeds diffusion current. At equilibrium the diffusion current density equals that of the drift current. Charge accumulation is related to the homogeneities of the material and the agglomeration of impurity ions by diffusion in the vicinity of electrodes or chemical changes in layers close to electrodes. The conductivity (σ_{dc}) of the crystal was calculated using the relation,

$$\sigma_{dc} = t / RA \tag{10}$$

where R is the measured resistance, t is the thickness of the sample and A is the area of the face in contact with the electrode. The above procedure was used to determine the DC electrical conductivity. The general relation for the temperature variation of conductivity is given by

$$\sigma_{dc} = \sigma_0 \exp[-\vec{E} / kT], \tag{11}$$

where σ_{dc} is a constant depending on material, $\vec{E}$ the activation of energy, T the absolute temperature and k the Boltzmann's constant. The above equation may be rewritten as

$$\ln \sigma_{dc} = \ln \sigma_0[-\vec{E} / kT], \tag{12}$$

A plot of σ_{dc} versus 1000/T gives - $\vec{E}$ /k as the slope and lnσ_{dc} as the intercept. The σ_{dc} values in the temperature region studied are found to increase with temperature for 4-methoxy benzoin crystal (Fig. 3 and Fig. 4). Electrical conductivity depends on thermal treatment of a crystal. Thus the conductivity at low temperatures depends on the cooling speed from melting point temperature to room temperature. Thus for slow cooling, the remaking of the lattice can occur by the migration of interstitials to vacancies, recombination of Schottky defects or migration of vacancies to the surface or along dislocation channels. On quenching or rapid cooling, a fraction of the vacancies freeze and the pre-exponential term includes a contribution from those frozen vacancies. The value of conductivity ln σ_{dc} is

found to increase with temperature. The plot of lnσT versus 1000/T is shown in Fig. 4. The activation energy calculated from the slope of the graph (Fig. 4) it is found to be 0.040 eV.

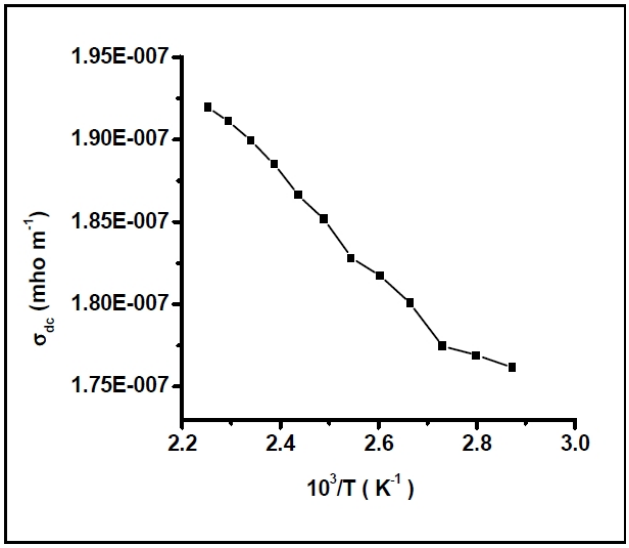

Fig. 3. Variation of dc conductivity with 1000/T for 4-methoxy benzoin crystal

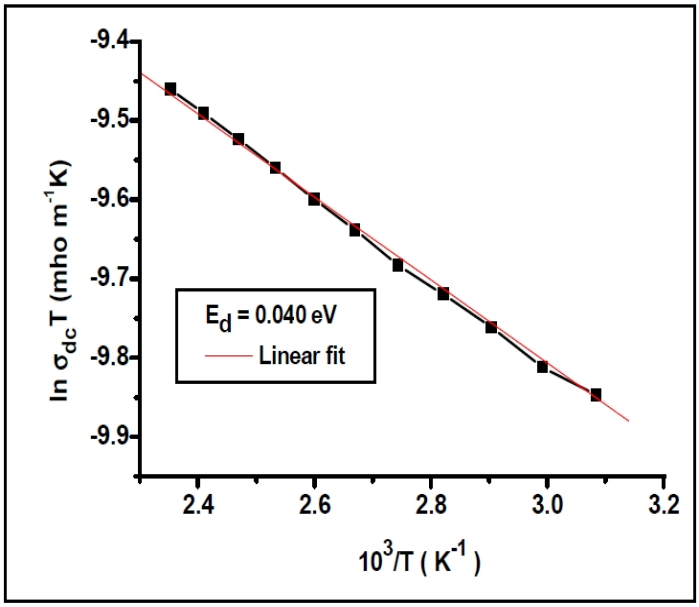

Fig. 4. Plot of ln(σ_{dc}) T versus 1000/T for 4-methoxy benzoin crystal

3.4 Photoconductivity Property

Photoconductivity studies have been carried out using Keithley 485 picoammeter instrument. The dark current has been recorded by keeping the crystal unexposed to any radiation.

Fig. 5 shows the variation of both dark current (I_d) and photocurrent (I_p) with applied electric field. It is seen from the plots that both I_d and I_p of the 4-methoxy benzoin crystal increase linearly with applied electric field. It is found from the plot that the dark current is always higher than the photo current, thus confirming the negative photoconductivity nature of the 4-methoxy benzoin crystal. The phenomenon of negative photoconductivity is explained by Stockmann model [20]. The negative photoconductivity in a solid is due to the decrease in the number of charge carriers or their lifetime, in the presence of radiation [21]. For a negative photoconductor, forbidden gap holds two energy levels in which one is placed between the Fermi level and the conduction band while the other is located close to the valence band. The second state has higher capture cross-section for electrons and holes. As it captures electrons from the conduction band and holes from the valence band, the number of charge carriers in the conduction band gets reduced and the current decreases in the presence of radiation.

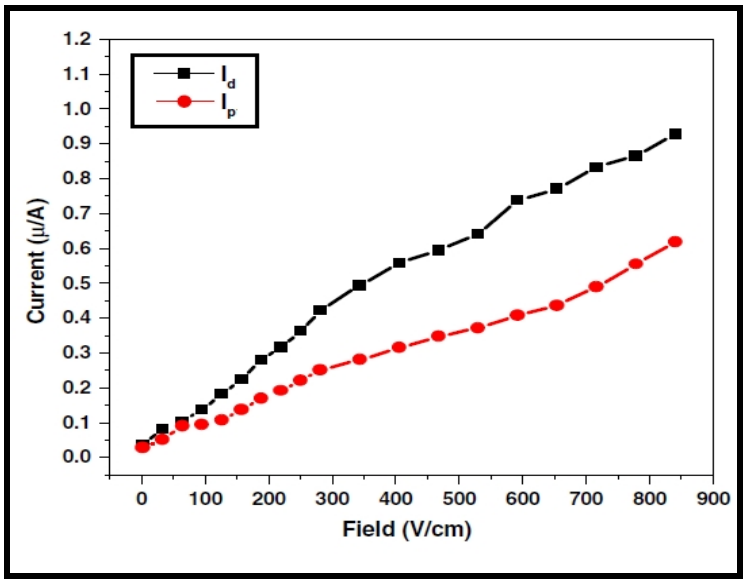

Fig. 5. Field dependent photoconductivity of 4-methoxy benzoin single crystal

4. CONCLUSION

The single crystals of 4-methoxy benzoin were grown by slow evaporation technique. The lattice parameters of the grown crystals are determined by single crystal XRD.The optical absorption spectrum analysis reveals that the crystal is transparent in the entire UV-VIS-NIR region with the lower cut-off wavelength as 400 nm. The optical bandgap for the grown crystal is found to be 3.50 eV. Optical constants such as optical band gap (E_g), absorption coefficient (α), refractive index (n), electric susceptibility χ_c and dielectric constants were calculated as a function of wavelength. The activation energy is determined from the plots of DC electrical conductivity. The photocurrent was less than the dark current, signifying negative photoconducting nature.

COMPETING INTERESTS

Author has declared that no competing interests exist.

REFERENCES

1. Jordon G, Kobayashi T, Blau WJ, Pfeiffer S, Horhold HH. Frequency up conversion of 800 nm ultra short pulses by two-photon absorption in a stilbenoid compound-doped polymer optical fiber. Advanced Functional Materials. 2003;13:751–754.
2. Yang Z, Aravazhi S, Schneider A, Seiler P, Jazbisnek M, Gunter P. Synthesis and crystal growth of stilbazolium derivatives for second-order nonlinear optics. Advanced Functional Materials. 2005;15:1072–6.
3. Kwon OP, Kwon SJ, Jazbisnek M, Brunner FDJ, Seo JI, Hunziker C. Organic phenolic configurationally locked polyene single crystals for electro-optic and terahertz wave applications. Advanced Functional Materials. 2008;18:3242–50.
4. Wong MS, Bosshard C, Gunter P. Crystal engineering of molecular NLO materials. Advanced Functional Materials. 1997;9:837–42.
5. Kiran AJ, Kim HC, Kim K, Rotermund F, Ravindra HJ, Dharmaprakash SM. Superior characteristics of organic chalcone single crystals as efficient non- linear optical material.Applied Physics Letters. 2008;92:113307–10.
6. John Kiran A, Lee HW, Ravindra HJ, Dharmaprakash SM, Kim K, Lim H. Designing novel chalcone single crystals with ultra-fast nonlinear optical responses and large multiphoton absorption coefficients. Current Applied Physics. 2011;10:1290–6.
7. Bosshard C, Sutter K, Prgtre P, Hulliger J, Florsheimer M, Kaatz P. Organic nonlinear optical materials. Gordon and Breach Science Publishers; 1995.
8. Zyss J. Molecular nonlinear optics: materials, physics, devices. Boston: Academic Press; 1994.
9. Prasad PN, Williams JD. Introduction to nonlinear optical effects in molecules and polymers. New York, Wiley; 1990.
10. Chemla DS, Zyss J. Nonlinear optical properties of organic molecules and crystals. Orlando, Academic Press; 1987.
11. Bosshard C, Sutter K, Schlesser R, Gunter P. Electro-optic effects in molecular crystals. Journal of the Optical Society of America B. 1993;10:867–85.
12. Zyss J. Hyperpolarizabilities of substituted conjugated molecules. III. Study of a family of donor–acceptor disubstituted phenyl-polyenes. Chemical Physics. 1979;71:909–16.
13. Levine BF, Bethea CG, Thurmond CD, Lynch RT, Berstein JL, An organic crystal with an exceptionally large optical second harmonic coefficient: 2methyl4nitroaniline. Journal of Applied Physics. 1979;50:2523–7.
14. Prasad PN, Williams DJ. Introduction to nonlinear optical effects in organic molecules and polymers. New York, Wiley; 1991.
15. Thanujav G, Nithya G, Kanagam C. Growth and characterization of a new NLO material: 4-methoxy benzoin. Photonics letters of Poland. 2012;4(1):41-43.
16. Chawla AK, Kaur D, Chandra R, Structural and optical characterization of ZnO nanocrystalline films deposited by sputtering.Optical Mater. 2007;29:995
17. Eya DDO, Ekpunobi AJ, Okeke CE. Influence of Thermal Annealing on the Optical Properties of Tin Oxide Thin Films Prepared by Chemical Bath Deposition Technique. Acad. Open Internet J. 2006;17.
18. Gupta V, Mansingh A. Influence of post deposition annealing on the structural and optical properties of sputtered zinc oxide film. J. Appl. Phys. 1996;80:1063.
19. Gaffar MA, Abu El-Fadl A, Bin Anooz S. Influence of strontium doping on the indirect band gap and optical constants of ammonium zinc chloride crystals. Physica B. 2003;327:43-54.

20. Joshi VN, Photoconductivity, Marcel Dekker, New York; 1990.
21. Bube RH. Photoconductivity of solids, Wiley, New York; 1981.

Peer-review history:
The peer review history for this paper can be accessed here:
http://www.sciencedomain.org/review-history.php?iid=191&id=5&aid=1027